NXF1/p15 heterodimers are essential for mRNA nuclear export in Drosophila

A. Herold, T. Klymenko and E. Izaurralde

RNA 2001 7: 1768-1780

RNA (2001), *7*:1768–1780. Cambridge University Press. Printed in the USA.

DOI: 10.1017.S1355838201013565

NXF1/p15 heterodimers are essential for mRNA nuclear export in *Drosophila*

ANDREA HEROLD, TETYANA KLYMENKO, and ELISA IZAURRALDE
European Molecular Biology Laboratory, 69117 Heidelberg, Germany

ABSTRACT

The conserved family of NXF proteins has been implicated in the export of messenger RNAs from the nucleus. In metazoans, NXFs heterodimerize with p15. The yeast genome encodes a single NXF protein (Mex67p), but there are multiple *nxf* genes in metazoans. Whether metazoan NXFs are functionally redundant, or their multiplication reflects an adaptation to a greater substrate complexity or to tissue-specific requirements has not been established. The *Drosophila* genome encodes one p15 homolog and four putative NXF proteins (NXF1 to NXF4). Here we show that depletion of the endogenous pools of NXF1 or p15 from *Drosophila* cells inhibits growth and results in a rapid and robust accumulation of polyadenylated RNAs within the nucleus. Fluorescence in situ hybridizations show that export of both heat-shock and non-heat-shock mRNAs, as well as intron-containing and intronless mRNAs is inhibited. Depleting endogenous NXF2 or NXF3 has no apparent phenotype. Moreover, NXF4 is not expressed at detectable levels in cultured *Drosophila* cells. We conclude that Dm NXF1/p15 heterodimers only (but not NXF2-NXF4) mediate the export of the majority of mRNAs in *Drosophila* cells and that the other members of the NXF family play more specialized or different roles.

Keywords: mRNA export; nuclear export; NXF; NXT; p15; *small bristles*; TAP

INTRODUCTION

Messenger RNAs are exported from the nucleus as large ribonucleoprotein (mRNP) complexes composed of an RNA molecule and several distinct proteins. Their export occurs through nuclear pore complexes (NPCs) and is a receptor-mediated process (reviewed by Mattaj & Englmeier, 1998; Nakielny & Dreyfuss, 1999). Studies in yeast and in vertebrate cells aimed at identifying export receptors for mRNPs have converged on an evolutionarily conserved family of proteins known as the nuclear export factor (NXF) family (reviewed by Conti & Izaurralde, 2001). The yeast genome encodes a single NXF protein, Mex67p, but there are two *nxf* genes in *Caenorhabditis elegans* (Ce), four in *Drosophila melanogaster* (Dm) and five putative genes in *Homo sapiens* (Hs; Herold et al., 2000; Tan et al., 2000; Jun et al., 2001; Yang et al., 2001). Hs NXF1 is also known as TAP and will be referred to as TAP.

Proteins of the NXF family have several conserved structural domains. From the N- to the C-terminus these are: an RNP-type RNA-binding domain, a leucine-rich repeat (LRR) domain, a middle region showing sequence and structural similarities to the nuclear transport factor 2 (the NTF2-like domain) and a C-terminal region related to ubiquitin associated (UBA) domains (the UBA-like domain; Fig. 2A; Herold et al., 2000; Liker et al., 2000; Suyama et al., 2000; Fribourg et al., 2001).

The NTF2-like domains of TAP, Hs NXF2, and Hs NXF3 heterodimerize with the small protein p15, which is also related to NTF2 (Katahira et al., 1999; Herold et al., 2000; Fribourg et al., 2001), but the NTF2-like domain of *Saccharomyces cerevisiae* (Sc) Mex67p binds to Mtr2p (Santos Rosa et al., 1998; Strässer et al., 2000). Mtr2p is not related in sequence to p15 but might be its functional analog (Katahira et al., 1999; Fribourg et al., 2001). The NTF2-like domain of TAP bound to p15 and the UBA-like domain mediate binding to nucleoporins, the components of the NPC (Fribourg et al., 2001). The role of the NTF2- and UBA-like domains in nucleoporin binding is conserved in Hs NXF2, Ce NXF1, and Sc Mex67p (Bear et al., 1999; Herold et al., 2000; Kang et al., 2000; Strässer et al., 2000; Tan et al., 2000; Yang et al., 2001).

NXF proteins not only share a similar structural domain organization, but at least five members of the NXF family exhibit RNA export activity or have been shown to participate directly in the export of mRNA to

Reprint requests to: Elisa Izaurralde, European Molecular Biology Laboratory, Meyerhofstrasse 1, 69117 Heidelberg, Germany; e-mail: izaurralde@embl-heidelberg.de.

the cytoplasm. This suggests that NXFs represent a family of RNA export factors. However, a different function cannot be excluded. Indeed, whereas Sc Mex67p and Ce NXF1 are essential for the export of bulk polyadenylated RNAs [poly(A)$^+$ RNA] (Segref et al., 1997; Tan et al., 2000), the function of Ce NXF2 is unknown, and its knockdown has no apparent phenotype (Tan et al., 2000).

TAP has been identified as the cellular protein recruited by the constitutive transport element (CTE) of simian type D retroviruses to promote the nuclear export of viral transcripts (Grüter et al., 1998). In *Xenopus laevis* oocytes, titration of TAP with an excess of CTE RNA blocks the export of cellular mRNAs (Pasquinelli et al., 1997; Saavedra et al., 1997). This, and the observation that coexpression of TAP and p15 in *S. cerevisiae* partially restores growth of the otherwise lethal *mex67/mtr2* double knockout (Katahira et al., 1999), strongly suggests a role for TAP in mRNA export. Consistently, overexpression of TAP/p15 heterodimers in human cultured cells, or microinjection of the recombinant proteins in *Xenopus laevis* oocytes, stimulates export of RNAs that are otherwise exported inefficiently (Braun et al., 2001). In addition, TAP/p15 heterodimers elicit nuclear export when either of them is tethered directly to a precursor mRNA that is normally retained within the nucleus (Braun et al., 2001; Guzik et al., 2001; Yang et al., 2001).

Despite the wealth of accumulated information, however, the identification of cellular mRNAs exported by TAP has remained elusive. The multiplication of *nxf* genes in metazoans has raised the question as to whether these proteins are functionally redundant or are specialized to export specific mRNA classes. Hs NXF2 is 58% identical to TAP and its coexpression with p15 in cultured cells also promotes the nuclear exit of inefficiently exported RNAs (Herold et al., 2000). Also, in the presence of p15, Hs NXF2, and NXF3 both promote export when tethered directly to an inefficiently spliced precursor mRNA (Yang et al., 2001; A. Herold & E. Izaurralde, unpubl. results). Thus, at least three out of five Hs NXFs exhibit RNA export activity. In *Drosophila*, at least two out of four NXF proteins (NXF1 and NXF2) have all the structural domains characteristic of the NXF family (Herold et al., 2000) and are expected a priori to be implicated in mRNP export.

In addition to the roles of the different NXFs in metazoans, the role of p15 is an open question in the mRNA export pathway. Based on the homology of p15 with NTF2, it has been reported that p15 binds RanGTP and is implicated in the export of tRNA and of substrates exported by CRM1 (Black et al., 1999, 2001; Ossareh-Nazari et al., 2001). Binding of p15 to Ran has not been reproduced in other laboratories (Katahira et al., 1999; Herold et al., 2000) and is incompatible with the known structure of the protein (Fribourg et al., 2001). The observation that p15 is required for the export of RNA mediated by TAP, NXF2, and NXF3, together with structural studies (Herold et al., 2000; Braun et al., 2001; Fribourg et al., 2001; Guzik et al., 2001), suggest that p15 forms a single structural and functional unit with the NTF2-like domains of the NXF proteins with which it heterodimerizes.

The emergence of double-stranded RNA interference (dsRNAi) technique, which has been applied successfully to deplete endogenous proteins from cultured *Drosophila* cells (Clemens et al., 2000), provides the opportunity to investigate the role of p15 and NXF proteins in vivo. Using this approach, we show that depletion of either NXF1 or p15 inhibits cell growth and results in a severe nuclear accumulation of poly(A)$^+$ RNA. In contrast, depletion of NXF2 or NXF3 has no apparent phenotype. We conclude that NXF1/p15 heterodimers are essential for the export of bulk mRNA in *Drosophila* cells. The other NXF homologs are likely to play more specialized roles, perhaps reflecting the greater substrate diversity of metazoa.

RESULTS

Drosophila NXF1–3 are expressed in different cell lines and throughout embryogenesis

The multiplication of the *nxf* genes in metazoans compared to yeast may reflect a redundancy in the mRNA export pathway or an adaptation to tissue- or substrate-specific requirements. To distinguish between these possibilities, we have analyzed the expression patterns of Hs and Dm NXFs. To this end, we have isolated full-length cDNAs encoding Dm NXF1, NXF2, NXF3, and p15 and a partial cDNA encoding Dm NXF4. Isolation and characterization of Hs NXFs and p15 was reported previously (Herold et al., 2000; Jun et al., 2001). Multiple tissue northern blot analysis shows that only TAP and the two Hs p15 homologs are ubiquitously expressed (Fig. 1A and data not shown). NXF2 is mainly expressed in testis (Fig. 1A). NXF3 is detected at a high level in testis and at low level in kidney (Fig. 1A). NXF5 is not detectable by northern blot but it could be amplified by PCR on cDNA derived from human fetal brain (Jun et al., 2001). Similar expression patterns were previously reported for TAP (Yoon et al., 1997) and recently for Hs NXFs (Jun et al., 2001; Yang et al., 2001). These expression patterns suggest that Hs NXF2–5 have tissue-specific functions and are unlikely to act as general export receptors of bulk mRNA.

The expression pattern of Dm NXFs was investigated by RT-PCR in different cell lines and in *Drosophila* embryos at different stages of development (Fig. 1B). NXF1–3 cDNAs could be amplified from all samples tested (Fig. 1B, lanes 1–5). The amplification was specific, as no product was obtained when the reverse transcriptase was omitted (Fig. 1B, lanes 6–10). More-

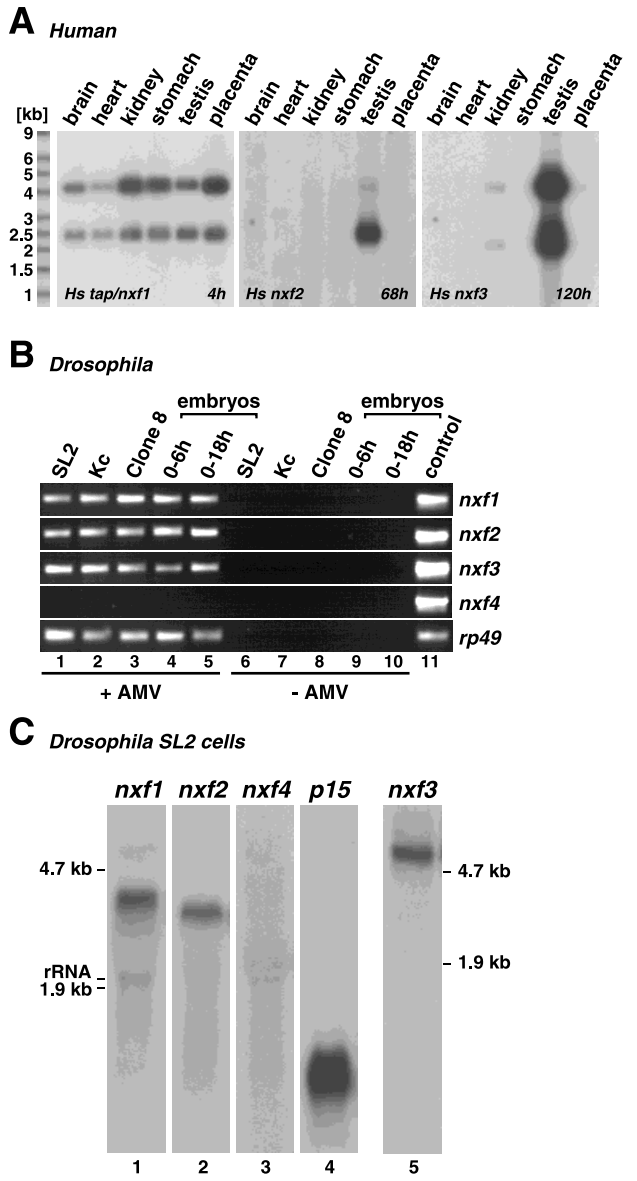

FIGURE 1. Comparison of Hs and Dm NXFs expression patterns. **A:** Tissue-specific expression pattern of TAP, Hs NXF2, and Hs NXF3. A human multiple tissue northern blot was consecutively hybridized with specific probes, as indicated. The exposure times are indicated on the right of each panel. **B:** The expression of Dm NXFs was investigated by semiquantitative RT-PCR on total RNA isolated from the embryonic cell lines SL2 and Kc, the Imaginal Disc cell line (clone 8), and embryos at different stages of development. **C:** Detection of Dm *nxfs* and *p15* mRNAs by northern blot analysis. Twenty micrograms of total RNA from SL2 cells were loaded in lanes 1–4 and 30 μg in lane 5. For *nxf4,* no signal was detected even after prolonged exposures.

over, the amplicons had the mobility of the product obtained when plasmids containing the corresponding cDNAs were used as templates (Fig. 1B, lane 11). No *nxf4* product was obtained using two different primer sets after 25 cycles of amplification. This indicates that *nxf4* mRNA represents a low-abundance transcript. The results obtained by RT-PCR were confirmed for *Drosophila* Schneider cells (SL2 cells) by northern blot analysis (Fig. 1C). Moreover, in situ analysis indicates that Dm NXF1–3 are expressed ubiquitously throughout embryonic development, whereas no signal above background levels is detected for *nxf4* (Korey et al., 2001; Wilkie et al., 2001; data not shown; C. Korey and D. van Vactor, pers. comm.).

Domain organization of *Drosophila melanogaster* NXF homologs

Comparison of the deduced amino acid sequence of Dm NXFs with TAP reveals that Dm NXF1 is more closely related to TAP than to the other Dm NXF homologs. Indeed, Dm NXF1 displays 35% sequence identity with TAP and about 20% identity with Dm NXF2–4. In addition, whereas Hs NXFs are at least 50% identical to each other (Herold et al., 2000), Dm NXFs are less well conserved and display about 20% sequence identity with any other Dm NXF.

Despite the divergence in the amino acid sequences, the overall domain organization of Dm NXFs is similar to that of TAP and other members of the NXF family. The LRR and the NTF2-like domains are present in NXF1, NXF2, and NXF3 (Fig. 2A). The C-terminal UBA-like domain is also present in NXF1 and NXF2 but has diverged in NXF3. In particular, a conserved tryptophane residue (W594 in TAP; Herold et al., 2000; Suyama et al., 2000) is not present in Dm NXF3. NXF4 lacks the NTF2-like and the UBA-like domains mediating the direct association with the NPC (Fribourg et al., 2001). The noncanonical RNP-type RNA-binding domain (RBD) and the N-terminal sequences upstream of the RBD are less well conserved. In NXF2, these sequences are predicted to contain additional LRRs.

The NTF2-like domain of Hs NXF proteins binds to p15 and is required for NXF function (Braun et al., 2001; Fribourg et al., 2001). We therefore investigated whether Dm NXF proteins interact with Dm p15. [^{35}S]methionine-labeled NXF1, NXF2, and NXF3 were synthesized in vitro in rabbit reticulocyte lysates and assayed for binding to glutathione agarose beads coated with Dm or Hs p15 fused to glutathione S-transferase (GST). NXF1 and NXF3 were selected on beads coated with either of the p15 proteins (Fig. 2B, lanes 3 and 4) but not on control beads coated with GST (Fig. 2B, lane 2). Dm NXF2 exhibits low affinity for p15. TAP displays a species-specific interaction profile, as it binds preferentially to Hs p15. As expected, the C-terminal domain of TAP (fragment 371–619), but not its N-terminal half (fragment 1–372), bound to Hs p15.

The subcellular localization of Dm NXF1, NXF2, and p15 fused to an HA-tag was investigated in transfected SL2 cells and compared to the localization of the endogenous nuclear protein Dm REF1 (Stutz et al., 2000). HA-tagged NXF1 and p15 were evenly spread throughout the nucleoplasm and were excluded from the nucleolus (Fig. 2C). Depending on the expression level,

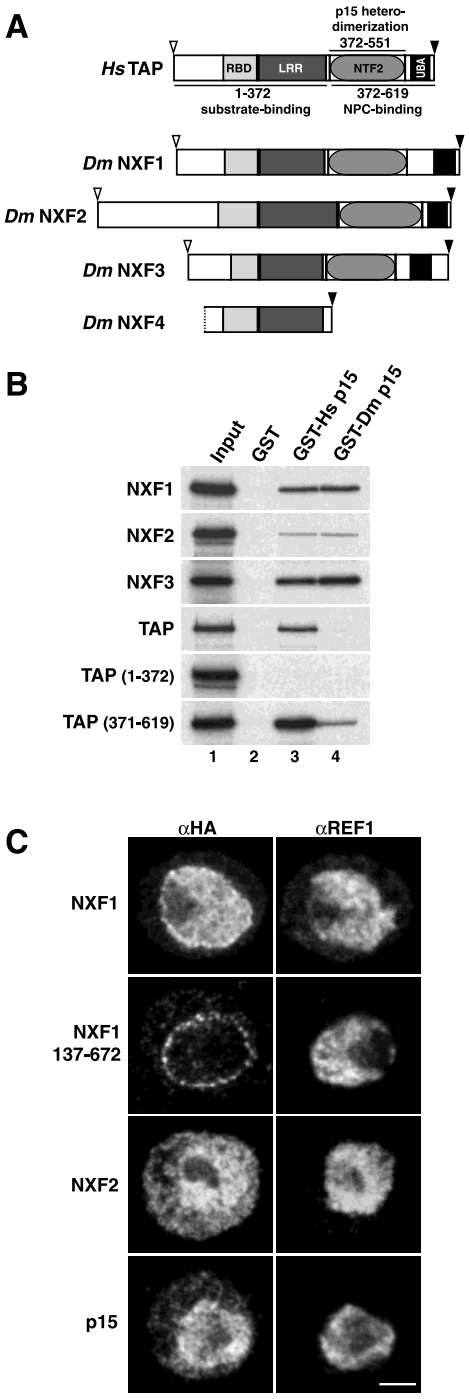

FIGURE 2. Domain organization and subcellular localization of Dm NXFs. **A:** RBD: noncanonical RNP-type RNA binding domain; LRR: leucine-rich repeat domain; NTF2: NTF2-like domain; UBA: UBA-like domain; open triangles: initiation codon; black triangles: stop codon. NXF4 sequence lacks the 5′ end. **B:** Dm NXF1 and Dm NXF3 interact with Dm p15 in vitro. GST-pull-down assays were performed with in vitro synthesized, [^{35}S]methionine-labeled proteins indicated on the left of the panels, and recombinant GST or GST fused to Hs or Dm p15 as indicated above the lanes. One-tenth of the input (lane 1) and one-quarter of the bound fractions (lanes 2–4) was analyzed by SDS-PAGE and fluorography. Analysis of the supernatants ensured that proteins were not degraded during the experiment (not shown). **C:** SL2 cells were transfected with plasmids expressing HA fusions of NXF1, NXF2, p15, and a N-terminal truncation of NXF1 (137–672), as indicated on the left. HA-tagged proteins were visualized by indirect immunofluorescence. Cells were double-labeled with anti-REF1 antibodies. Scale bar = 2.5 μm.

p15 could also be detected in the cytoplasm (Fig. 2C). As reported for TAP and Hs p15, a fraction of Dm NXF1 and Dm p15 associated with the nuclear envelope. Nuclear envelope association mediated by the C-terminal domain of TAP can be clearly visualized by deleting the N-terminal nuclear localization signal. This reduces the nuclear uptake of the protein and the nucleoplasmic signal (Bachi et al., 2000). The nuclear envelope association of Dm NXF1 was confirmed by deleting the N-terminal sequences upstream of the RBD (NXF1 137–672). The truncated protein was localized predominantly at the nuclear rim in a punctuate pattern (Fig. 2C), suggesting that Dm NXF1 binds to nucleoporins in vivo. Dm NXF2 was detected in both the nucleoplasm and the cytoplasm (Fig. 2C). Thus, despite the fact that NXF2 contains all structural domains characteristic of NXF proteins, it has low affinity for p15 and does not clearly localize at the nuclear rim.

Depletion of NXF1 and p15 proteins by dsRNAi inhibits cell growth

To deplete endogenous Dm p15 and NXF1–4, SL2 cells were transfected with dsRNAs corresponding to N-terminal fragments of the proteins. As a control, a dsRNA corresponding to an N-terminal fragment of green fluorescent protein (GFP) was transfected. Strikingly, depletion of NXF1 and p15 results in a dramatic inhibition of cell growth as early as 2 days after transfection (Fig. 3A), indicating that these proteins are essential. Depletion of NXF2–4 has no effect on cell growth compared to untreated cells or cells transfected with GFP dsRNA (Fig. 3A).

To determine the efficiency and specificity of the depletion, we transfected dsRNAs corresponding to NXF1, NXF2, and p15 into SL2 cells and performed a time-course western blot analysis with antibodies raised against the recombinant proteins. Only 2 days after transfection, the steady-state expression levels of NXF1 and NXF2 were already reduced to about 10 to 20% of the levels detected in untreated cells (Fig. 3B, day 2 versus day 0), whereas p15 levels were reduced down to 20–30%. No recovery of the protein expression levels was observed even 8 days after transfection (Fig. 3B). The depletion is specific for the following reasons. First, the expression level of an unrelated protein, the translation initiation factor eIF4G, was not affected by NXF1, p15, or NXF2 dsRNAs (Fig. 3B). Second, transfection of the unrelated GFP dsRNA had no effect on the expression of any of the proteins tested (Fig. 3C, lanes 1 and 2). More importantly, NXF1 protein levels are not affected in cells transfected with NXF2 dsRNA. Similarly, NXF2 expression levels are unaffected in cells transfected with NXF1 or control (GFP) dsRNA (Fig. 3C). In the absence of specific antibodies directed to NXF3, the efficiency of NXF3 depletion was determined by northern blot (Fig. 3D). The

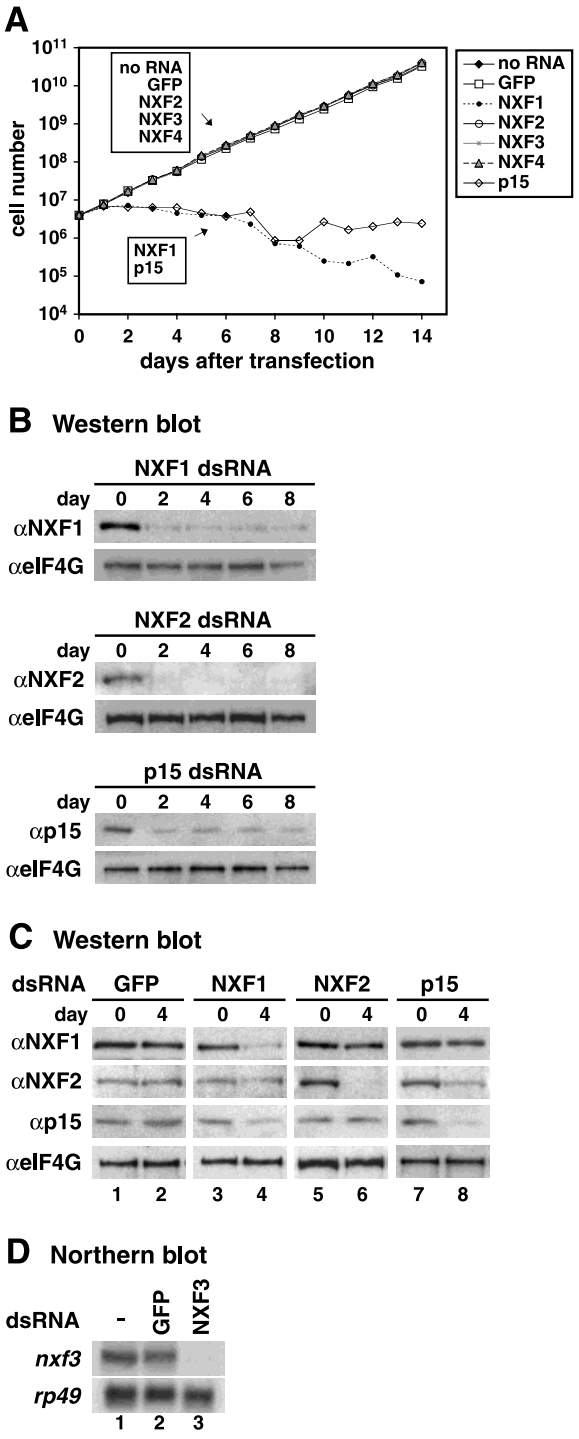

FIGURE 3. Depletion of NXF1 and p15 inhibits cell growth. **A:** SL2 cells growing in suspension were transfected with dsRNA specific for NXF1–4, p15, or GFP. Cell numbers were determined every day. On days 4 and 8, cells were retransfected with NXF2–4 and GFP dsRNAs. **B:** Two to 8 days after transfecting the indicated dsRNAs, SL2 cells were analyzed by western blotting with antibodies raised against recombinant NXF1, NXF2, p15, and the unrelated protein eIF4G as a control. **C:** The depletion of NXF1 and NXF2 is specific. SL2 cells were transfected with GFP, NXF1, NXF2, or p15 dsRNA as indicated above the lanes. Four days after transfection NXF1, NXF2, p15, and eIF4G protein levels were analyzed by western blotting of total cell lysates. **D:** Six days posttransfection, total RNA isolated from SL2 cells from the same experiment as in **A** was analyzed for the presence of *nxf3* mRNA by northern blot. The same filter was probed for the presence *rp49* mRNA.

nxf3 mRNA was degraded in cells transfected with the corresponding dsRNA (Fig. 3D, lane 3). Transfection of GFP dsRNA does not affect *nxf3* mRNA levels (Fig. 3D, lane 2). The effect of NXF3 dsRNA is specific, as the mRNA coding for the ribosomal protein rp49 was not degraded (Fig. 3D, lower panel).

In transiently transfected human 293 cells, the steady-state expression level of TAP is increased when Hs p15 is cotransfected (Herold et al., 2000; Braun et al., 2001). Therefore we tested if the marked growth defect observed in cells depleted of p15 was indirect and caused by NXF1 destabilization or mislocalization. As shown in Figure 3C, NXF1 protein is not destabilized in cells that have been depleted of p15 (lanes 7–8). Even 1 week after transfection of p15 dsRNA, the steady-state expression level of NXF1 was not reduced (not shown). NXF2, in contrast, was partially destabilized in cells depleted of p15 (Fig. 3C, lanes 7–8) suggesting that despite a weak binding in vitro (Fig. 3C), these proteins may form heterodimers in vivo. Unexpectedly, expression of p15 was slightly but reproducibly reduced in cells depleted of NXF1 (Fig. 3C, lanes 3–4).

The subcellular localization of HA-tagged Dm NXF1 and NXF2 did not change when transiently expressed in cells depleted of p15. HA-tagged p15 also remained predominantly nuclear in cells depleted of NXF1 (data not shown). Because NXF1 is neither destabilized nor mislocalized in cells depleted of p15, we conclude that in the absence of p15, NXF1 cannot perform its essential function.

Polyadenylated RNAs accumulate in the nucleus of cells depleted of NXF1 or p15

The intracellular distribution of bulk poly(A)$^+$ RNA in control cells and in cells depleted of NXF1–4 or p15 was investigated by in situ hybridization with a Cy3-labeled oligo(dT) probe. The nuclear envelope was stained with the monoclonal antibody mAb414, which recognizes several nucleoporins, or with fluorescently labeled wheat germ agglutinin (WGA).

At steady state, a large fraction of poly(A)$^+$ RNA is cytoplasmic in untreated SL2 cells or cells transfected with control GFP dsRNA (Fig. 4A, panel a; Fig. 4B, panels a and e). In contrast, NXF1 depletion results in a robust nuclear accumulation of poly(A)$^+$ RNAs (Fig. 4A, panel e; Fig. 4B, panel b). The poly(A)$^+$ signal is widespread within the nucleoplasm and is excluded from the large nucleolus characteristic of this cell line (Fig. 4A, panel e). This change in the distribution of poly(A)$^+$ RNA is also observed in cells depleted of endogenous p15 (Fig. 4A, panel m; Fig. 4B, panel c). The nuclear accumulation of poly(A)$^+$ RNA correlates with the depletion of the targeted proteins, as it is detected in about half or one-third of the cell population as early as 40 h after transfecting NXF1 or p15 dsRNAs,

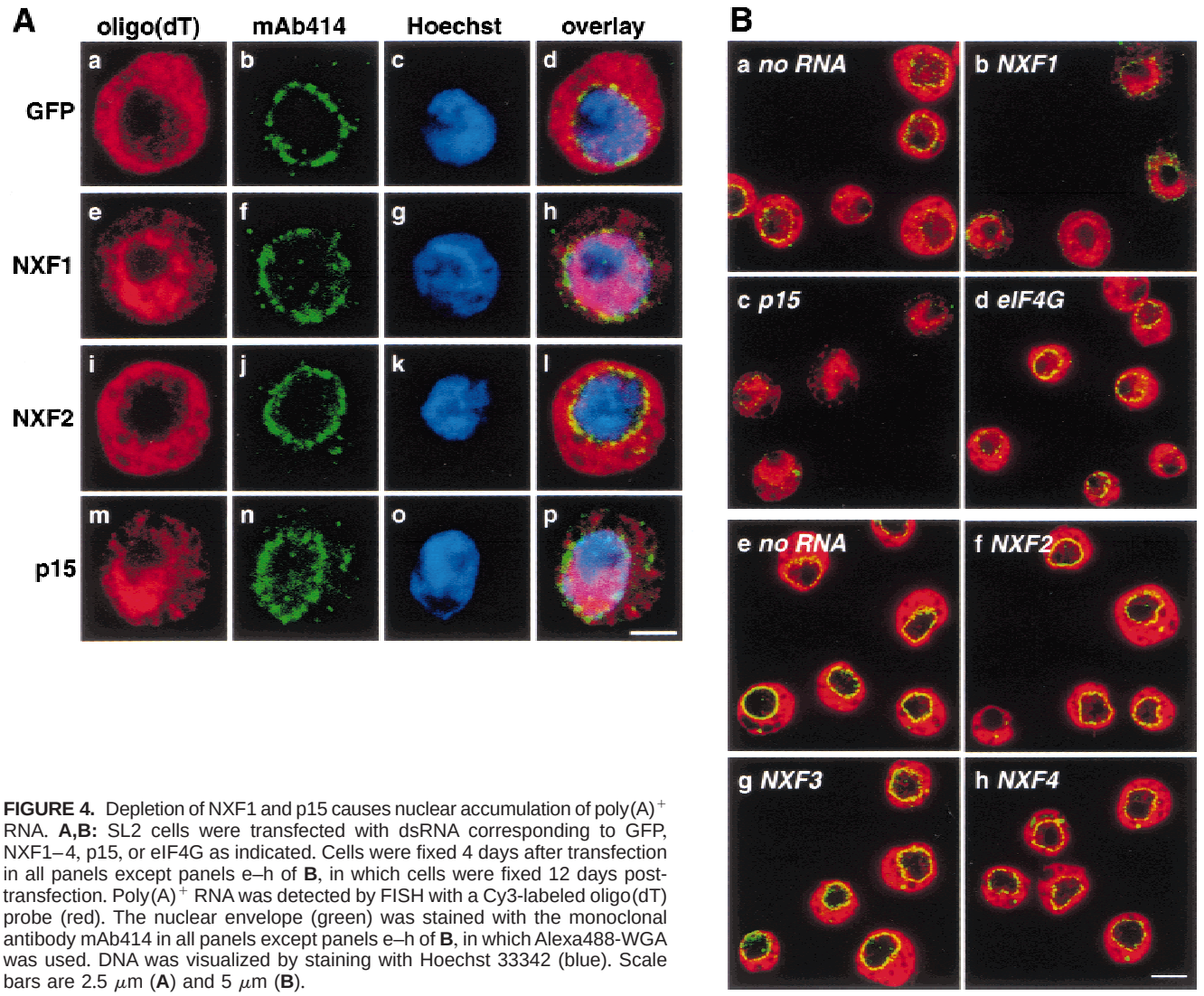

FIGURE 4. Depletion of NXF1 and p15 causes nuclear accumulation of poly(A)$^+$ RNA. **A,B:** SL2 cells were transfected with dsRNA corresponding to GFP, NXF1–4, p15, or eIF4G as indicated. Cells were fixed 4 days after transfection in all panels except panels e–h of **B**, in which cells were fixed 12 days post-transfection. Poly(A)$^+$ RNA was detected by FISH with a Cy3-labeled oligo(dT) probe (red). The nuclear envelope (green) was stained with the monoclonal antibody mAb414 in all panels except panels e–h of **B**, in which Alexa488-WGA was used. DNA was visualized by staining with Hoechst 33342 (blue). Scale bars are 2.5 μm (**A**) and 5 μm (**B**).

respectively (data not shown). The accumulation can be observed in almost all cells 65 h after transfection.

In cells depleted of NXF2–4, poly(A)$^+$ RNAs localize mainly to the cytoplasm, as in control cells (Fig. 4A, panel i; Fig. 4B, panels f–h). Thus, in the presence of NXF1, depletion of NXF2–4 does not affect the export of bulk poly(A)$^+$ RNA. Moreover, the fact that NXF2 protein is present in cells depleted of NXF1 (Fig. 3C, lanes 3 and 4), but does not restore cell growth or poly(A)$^+$ mRNA export, suggests that these proteins are not functionally redundant. Alternatively, the expression levels of NXF2 or of NXF3 in SL2 cells might not be sufficient to compensate for the depletion of NXF1. Quantitative western blots indicate that NXF2 is indeed, about four times less abundant than NXF1 in SL2 cells. However, overexpression of NXF2, with or without p15, does not rescue the NXF1-knockdown phenotype (data not shown).

The nuclear accumulation of poly(A)$^+$ RNA observed in cells depleted of NXF1 and p15 is not a direct consequence of the inhibition of cell growth, as depletion of eIF4G also results in a strong growth defect, which is not accompanied by a nuclear accumulation of poly(A)$^+$ RNA (Fig. 4B, panel d). Together, our data suggest that the growth arrest observed in cells depleted of NXF1 or p15 is a consequence of a general block to mRNA export.

Depletion of NXF1 or p15 results in a general block of protein synthesis

The general inhibition of mRNA export in SL2 cells depleted of NXF1 or p15 was confirmed by metabolic labeling (Fig. 5A). Cells depleted of NXF1, NXF2, or p15 were pulse labeled with [^{35}S]methionine 4 days after transfecting the corresponding dsRNAs. Total lysates from equivalent numbers of cells were analyzed by SDS-PAGE and fluorography. The incorporation of [^{35}S]methionine into newly synthesized proteins was reduced in cells depleted of NXF1 or p15 in compari-

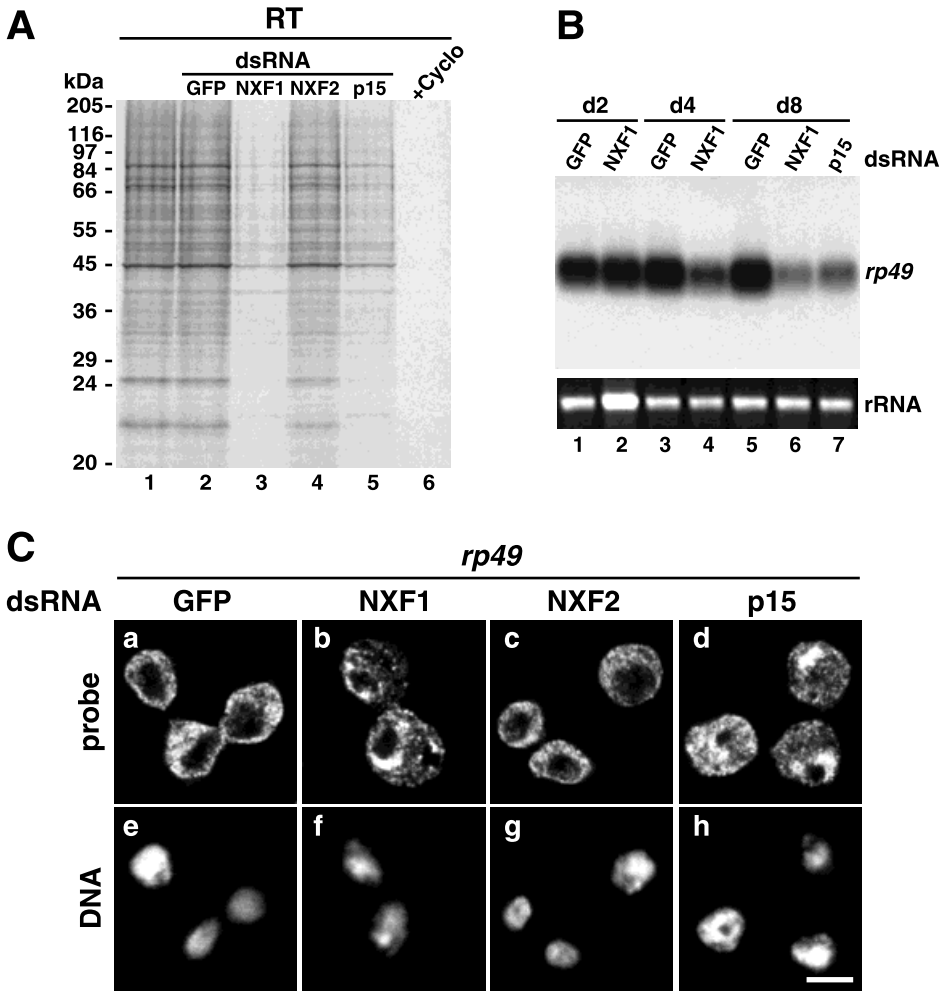

FIGURE 5. Depletion of NXF1 and p15 results in a general block of protein synthesis and leads to nuclear accumulation of *rp49* mRNA. **A:** SL2 cells were transfected with GFP, NXF1, NXF2, and p15 dsRNA. Four days after transfection, cells were pulse labeled with [^{35}S]methionine for 1 h. Total-cell extracts were analyzed by SDS-PAGE followed by fluorography. [^{35}S]methionine incorporation is dramatically reduced in cells depleted of NXF1 or p15 (lanes 3 and 5), or when cyclohexamide (20 μg/mL) was included during the labeling reaction (lane 6). **B:** Northern blot analysis using a *rp49*-specific probe. SL2 cells were transfected with the indicated dsRNAs and total RNA was isolated 2 (lanes 1 and 2), 4 (lanes 3 and 4), or 8 (lanes 5–7) days after transfection. Five micrograms of total RNA were loaded per lane. The lower panel shows the corresponding rRNA stained with ethidium bromide. **C:** SL2 cells were transfected with indicated dsRNAs. Four days after transfection cells were fixed, and *rp49* mRNA was detected by FISH using a digoxigenin-labeled probe. **a**–**d**: rp49 signal; **e**–**h**: DNA staining. Scale bar = 5 μm.

son to control cells (Fig. 5A, lanes 3 and 5 versus 1 and 2). This inhibition of protein synthesis affects most proteins to a similar extent, suggesting that NXF1 and p15 are involved in the nuclear export of most mRNAs. No decline in protein labeling was observed in cells depleted of NXF2 (Fig. 5A, lane 4).

To investigate whether the inhibition of protein synthesis is caused by a block to mRNA export and not to transcription, we analyzed the expression level and the localization of *rp49* mRNA, which is an abundant mRNA in SL2 cells. Northern blot analysis showed that 4 days after transfection of NXF1 dsRNA, the expression levels of this message were reduced in comparison to the levels detected in control cells (Fig. 5B, lanes 3 and 4). Notably, 8 days after transfection, the steady-state expression levels of the *rp49* mRNA were strongly reduced in cells depleted of NXF1 or p15 in comparison to control cells (Fig. 5B, lanes 5–7). Whether this strong reduction in *rp49* mRNA level is caused by a change in the turnover of this mRNA or by a reduced transcriptional activity in cells in which mRNA export has been inhibited for 8 days has not been investigated.

The subcellular localization of the endogenous *rp49* mRNA was analyzed 4 days after transfection by FISH. The *rp49* mRNA was detected predominantly in the nucleus of 50–65% of cells depleted of NXF1 or p15 (Fig. 5C, panels b and d). In control cells and cells depleted of NXF2, the *rp49* message was found in the cytoplasm (Fig. 5C, panels a and c). Fluorescently labeled sense probe did not yield a signal over back-

ground when employed in the RNA–FISH procedure (not shown). These results indicate that the inhibition of protein synthesis is in part due to an mRNA export block in cells where NXF1 and p15 have been knocked down. A reduced transcriptional activity or an increased turnover of mRNAs that cannot exit the nucleus also contributes to the observed phenotype.

Inhibition of heat-shock response by depletion of NXF1 or p15

To investigate whether heat-shock mRNAs are also exported via the NXF1/p15 pathway, we followed the production of heat-shock proteins in cells depleted of NXF1 or p15 shifted to 33–37 °C. Incubation of cultured *Drosophila* cells at these elevated temperatures induces the massive transcription and translation of a set of well-characterized heat-shock genes, whereas production of non-heat-shock proteins is inhibited (reviewed by Echalier, 1997). This was observed in untreated cells and control cells transfected with GFP or NXF2 dsRNAs (Fig. 6A, lanes 1, 2, and 4). In cells depleted of NXF1 or p15, expression of heat-shock proteins was inhibited (Fig. 6A, lanes 3 and 5). Northern blot analyses showed that both in depleted and control cells *hsp70* mRNA was strongly induced after shifting the cells for 1 h to 37 °C (Fig. 6B, lanes 2, 4, and 6). This indicates that the inhibition of HSP70 protein synthesis in NXF1 or p15 depleted cells is not caused by a failure to transcribe the *hsp70* mRNA.

The levels of *hsp83* mRNA before and after heat shock at 33 °C or 37 °C were also analyzed. *hsp83* differs from all other heat-shock mRNAs in that it is normally expressed to relatively high levels even without exposure to heat stress, and in being the only heat-shock gene containing an intron (Echalier, 1997). When cells were shifted to 33 °C or 37 °C, *hsp83* mRNA synthesis was induced to comparable levels in control cells and cells depleted of NXF1 or p15 (Fig. 6C, lanes 2, 5, 8 and 3, 6, 9). As splicing is inhibited at 37 °C (Yost & Lindquist, 1986), the unspliced *hsp83* pre-mRNA was also detected after shifting the cells to this temperature (Fig. 6C, lanes 3, 6, and 9, asterisk). This accumulation of unspliced *hsp83* pre-mRNA occurs in depleted cells as well as in control cells at 37 °C, but was not observed in cells depleted of NXF1 or p15 at temperatures below 37 °C. Thus, the inability to express heat-shock proteins in cells depleted of NXF1 or p15 is not due to an inhibition of transcription or splicing of the corresponding mRNAs.

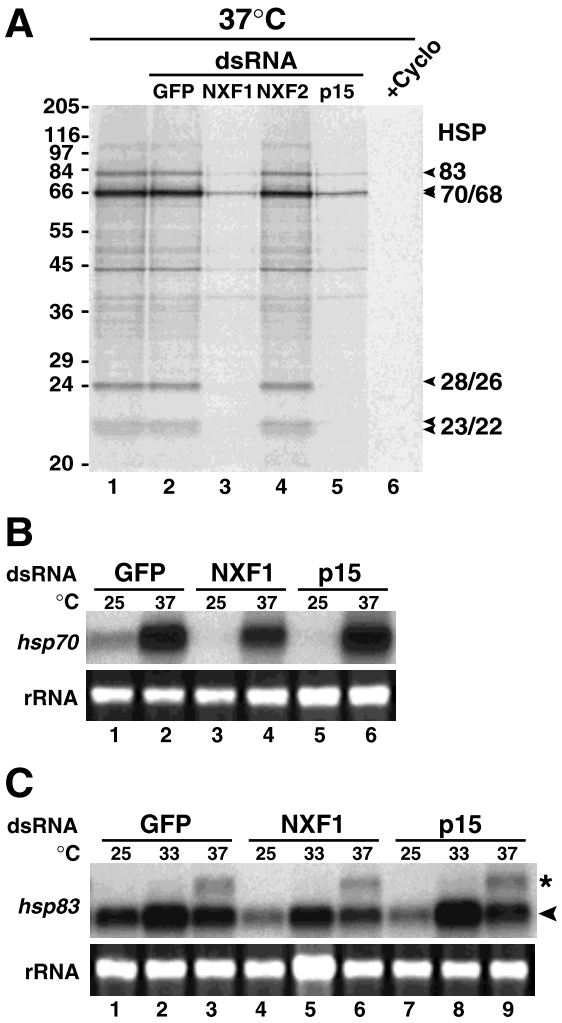

FIGURE 6. Cells depleted of NXF1 or p15 cannot produce heat-shock proteins. **A:** Four days after transfection with the indicated dsRNAs, SL2 cells were shifted to 37 °C and subjected to a metabolic pulse labeling as in Figure 5A. Total-cell extracts were analyzed by SDS-PAGE followed by fluorography. The heat-shock response is inhibited in cells depleted of NXF1 or p15 (lanes 3 and 5) or when cyclohexamide is present during the labeling reaction. **B,C:** SL2 cells were transfected with the indicated dsRNAs. Eight days after transfection, cells were either kept at 25 °C (lanes 1, 3, 5 in **B**; lanes 1, 4, 7 in **C**) or subjected to a 1-h heat shock at the indicated temperatures (lanes 2, 4, and 6 in **B**; lanes 2, 3, 5, 6, 8, and 9 in **C**). Five micrograms of total RNA was analyzed by northern blot using probes specific for *hsp70* or *hsp83* mRNAs. The lower panel shows the ethidium bromide stained ribosomal RNA. The asterisk indicates the position of the unspliced *hsp83* precursor mRNA that accumulates at 37 °C, and the fully spliced mRNA is indicated by an arrowhead.

Nuclear export of hsp70 and hsp83 mRNAs is inhibited in cells depleted of NXF1 or p15

The intracellular distribution of *hsp70* and *hsp83* mRNAs was determined in cells depleted of NXF1 or p15 by FISH. In control cells, the *hsp70* mRNA is detected mainly in the cytoplasm and the intensity of the signal increases when cells are shifted to 37 °C prior to fixation (Fig. 7A, panels a and e). In contrast, a clear nuclear accumulation of *hsp70* mRNA is observed in cells depleted of NXF1 or p15 (Fig. 7A, panels b and d). This accumulation was detected in more than 70% (NXF1) or 50% (p15) of the cells, respectively. The localization of *hsp70* mRNA in cells depleted of NXF2 is indistinguishable from that of control cells (Fig. 7A, panel c).

When *hsp83* mRNA FISH analysis was performed, the signals detected before and after heat shock did

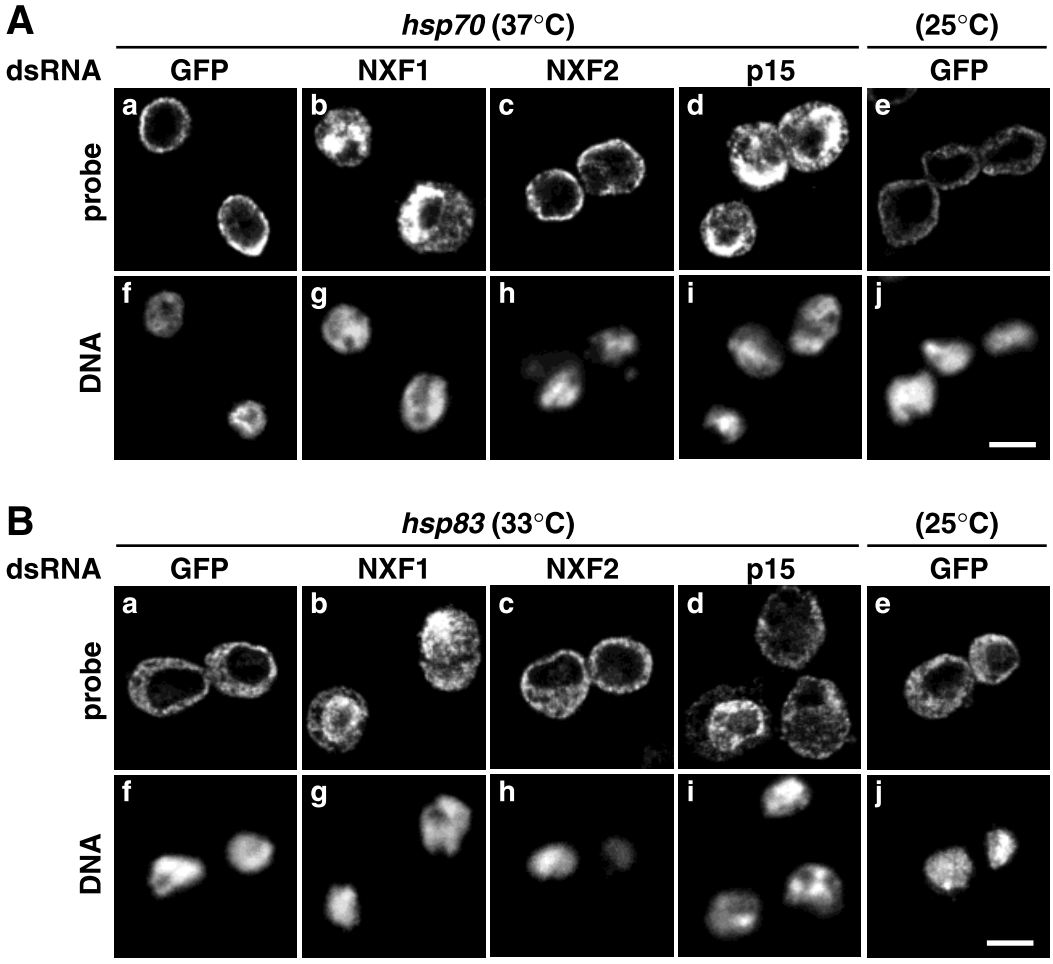

FIGURE 7. *hsp70* and *hsp83* mRNA accumulate in the nucleus of cells depleted of NXF1 or p15. **A:** SL2 cells were shifted to 37 °C for 1 h 4 days after transfecting the indicated dsRNAs. *hsp70* mRNA was detected by FISH using a digoxigenin-labeled RNA probe. **a**–**e**: *hsp70* signal; **f**–**j**: DNA staining. Scale bar = 5 μm. **B:** In situ hybridizations were performed with a probe specific for *hsp83* mRNA after shifting the cells 1 h to 33 °C. **a**–**e**: *hsp83* signal; **f**–**j**: DNA staining. *hsp83* mRNA is detected in cells before transcriptional induction at 33 °C (**e**).

not differ significantly in intensity (Fig. 7B, panels a and e), because this mRNA is already expressed at room temperature (Fig. 6C). The localization of *hsp83* mRNA was analyzed in cells depleted of NXF1 or p15 after transcriptional induction at 33 °C. Incubation at 37°C was avoided, because at this temperature, in addition to the cytoplasmic signal, a nuclear signal was observed even in control cells, most likely due to the inhibition of splicing (data not shown). After shifting the cells for 1 h to 33 °C, the *hsp83* mRNA localized to the cytoplasm of control cells (Fig. 7B, panel a). In cells depleted of p15 or NXF1, the distribution of *hsp83* mRNA changed significantly either to a predominantly nuclear localization (about 40% of the cells) or an even distribution between cytoplasm and nucleus (approximately 45% of the cells; Fig. 7B, panels b and d). Cells depleted of NXF2 show the same distribution as control cells (Fig. 7B, panel c). No signal over background was detected when sense probes were employed (not shown). Hence, we conclude that the lack of heat-shock protein synthesis in cells depleted of NXF1 or p15 is caused by the inability of heat-shock mRNAs to leave the nucleus.

DISCUSSION

In this study, we have investigated the role of *Drosophila* NXFs and p15 in mRNA nuclear export by specifically depleting these proteins by dsRNAi. We show that although NXF2–4 knockdowns have no apparent phenotype, depletion of either NXF1 or p15 inhibits cell growth and results in a robust nuclear accumulation of bulk poly(A)$^+$ RNA. Because the steady-state expression level of NXF1 is not affected in cells depleted of p15, we conclude that both NXF1 and p15 are essential for mRNA nuclear export. This together with previous biochemical, structural, and functional studies (Katahira et al., 1999; Suyama et al., 2000; Braun et al., 2001; Fribourg et al., 2001; Guzik et al., 2001), indicates that the two proteins act as heterodimers. We

also show that, contrary to expectation, the majority of mRNAs are exported by NXF1/p15 heterodimers and the multiplication of *nxf* genes in higher eukaryotes does not reflect a redundancy in the export pathway of bulk mRNA.

mRNA export in *Drosophila* is mediated by NXF/p15 heterodimers

The nuclear accumulation of poly(A)$^+$ RNA in cells depleted of NXF1 or p15 correlates well with the reduction of the endogenous protein levels and the cell growth arrest (Figs. 3 and 4) and is similar to the phenotype described in *S. cerevisiae* haploid strains carrying conditional mutations in *mex67* or *mtr2* (Kadowaki et al., 1994; Segref et al., 1997; Santos Rosa et al., 1998). A block to mRNA export in *S. cerevisiae* leads to hyperadenylation of the transcripts accumulating in the nucleus (Hilleren & Parker, 2001; Jensen et al., 2001). This implies that the nuclear signals detected by oligo(dT) in situ hybridizations following export inhibition may not necessarily correlate with the efficiency of the export block. However, in yeast cells carrying mutations in *mex67*, the results obtained by FISH with oligo(dT) were confirmed for individual mRNAs using specific probes. In particular, ASH1 mRNA, PGK1 mRNA, and heat-shock mRNAs have been shown to accumulate in the nucleus in *mex67* conditional mutants at the restrictive temperature (Hurt et al., 2000; Vainberg et al., 2000; Jensen et al., 2001). Inhibition of heat-shock mRNA export was also confirmed by the absence of heat-shock protein synthesis in these cells following heat stress (Hurt et al., 2000; Vainberg et al., 2000; Jensen et al., 2001).

We have not investigated whether hyperadenylation occurs in *Drosophila* cells following mRNA export inhibition. Nevertheless, we can exclude the possibility that the nuclear signal detected in cells depleted of NXF1 or p15 using an oligo(dT) probe is due only to hyperadenylation of nascent transcripts, because FISH analysis using probes to detect specific mRNAs show that these mRNAs were indeed mislocalized in these cells. Moreover, the inhibition of protein labeling in cells depleted of NXF1 or p15 suggests that export of most mRNAs is affected. In addition, heat-shock protein synthesis is eliminated in cells depleted of NXF1 or p15. Our data indicate that Dm NXF1/p15 heterodimers are essential for the export of heat-shock and non-heat-shock mRNAs. The fact that export of an intronless mRNA (*hsp70*) and of intron-containing mRNAs (i.e., *hsp83* and *rp49*) is inhibited, indicates that Dm NXF1/p15 heterodimers mediate export of both spliced and intronless mRNAs as previously suggested for TAP/p15 (Braun et al., 2001; Rodrigues et al., 2001). Consistently, in the accompanying manuscript by Wilkie et al. (2001), it is shown that Dm NXF1 is the ubiquitous mRNA export receptor required in all tissues and stages of development.

Dm NXF1 is encoded by the *Drosophila* gene *small bristles* (*sbr*), for which multiple alleles have been described. Mutations in this gene affect several tissues during *Drosophila* development including the morphogenesis of embryonic neurons and muscles. Moreover, adult flies have smaller and thinner sensory bristles and are defective in the development of the female germ line and/or in spermatogenesis. These tissue-specific effects of *sbr* alleles are likely to reflect an increased sensitivity to a reduction in mRNA export and therefore in protein synthesis in these tissues (Korey et al., 2001; Wilkie et al., 2001, and references therein).

NXF1/p15 form a single functional unit

Crystallographic studies on the NTF2-like domain of TAP bound to p15 indicate that these proteins form a single structural unit (Fribourg et al., 2001). Our data indicate that Dm NXF1/p15 form a single functional unit and cannot promote export in the absence of the other subunit of the heterodimer. However, although the NTF2-like domain of NXFs is conserved, p15 is not. In *S. cerevisiae*, Mex67p heterodimerizes with Mtr2p (Santos Rosa et al., 1998; Strässer et al., 2000). The lack of sequence conservation between Mtr2p and p15 is compatible with a structural role for these proteins, such as allowing the proper folding of the NTF2-like domains of NXFs, which in turn mediates binding to the NPC (Fribourg et al., 2001). Whether p15 or Mtr2p contribute not only to NPC association but also to cargo binding is an open question. It is interesting to note that the fact that NXFs are functional only as heterodimers with p15 or Mtr2p could provide a mechanism for regulating their activity.

Role of *nxf* genes in metazoans: Tissue-specific or housekeeping functions?

In this study, we show that Dm NXF2–4 cannot sustain growth or export of bulk mRNA in cells depleted of NXF1. A possible explanation for this observation is that the physiological expression levels of NXF2–4 may be insufficient to restore export. This is indeed the case for NXF4, which is either not expressed or expressed at very low levels in SL2 cells and in *Drosophila* embryos. The expression level of Dm NXF2 is approximately fourfold lower than that of NXF1, and thus similar to the levels of NXF1 protein after depletion. However, overexpression of Dm NXF2 does not rescue NXF1-knockdown (data not shown). These results together with the divergence of NXF2–4 sequences point to a nonredundant function.

Dm NXF1 is expressed in all tissues and in all developmental stages (Korey et al., 2001; Wilkie et al.,

2001). Similar to *nxf1*, *nxf2*, and *nxf3* mRNAs are expressed in different *Drosophila* cell lines and are evenly detected in *Drosophila* embryos throughout development (Fig. 1B; C. Korey & D. Van Vactor, pers. comm.). This suggests that Dm NXF2–3 may have a housekeeping role, although a tissue-specific pattern of expression in adult flies cannot currently be ruled out. In contrast, Hs NXF2, NXF3, and NXF5 exhibit a tissue-specific expression pattern. Whether Hs or Dm NXFs promote export of specific transcripts in cells where they are expressed needs to be established, but it is also possible that some of these proteins may have a different function. The divergence of Dm NXF2–4 relative to Hs NXF2–5 and their different expression patterns indicates that the role of these proteins in vivo can only be accessed in the homologous systems.

MATERIALS AND METHODS

Cloning of *nxf*s and p15 cDNAs

The prediction of genes encoding Dm NXF and p15 homologs has been reported previously (Herold et al., 2000). The corresponding cDNAs were amplified by PCR using a *Drosophila* embryonic cDNA library or *Drosophila melanogaster* quick-clone cDNA (Clontech). All PCR reactions were performed with the Expand™ high-fidelity PCR system (Roche). The amplified cDNAs were cloned into a derivative of pBS-SK (pBS-SKHA) and sequenced. These cDNAs were used for all further subcloning steps. NXF1 is the product of the gene known as *small bristles* (Korey et al., 2001; Wilkie et al., 2001; accession numbers AJ251947 and AJ318090). The NXF2 sequence data has been submitted to the European Molecular Biology Laboratory (EMBL) database under accession number AJ312282 and is identical to the prediction in the Flybase (gene CG4118). Full-length p15 cDNA was amplified by PCR and is identical to the sequence of Dm NXT1 (accession number AF156959).

The NXF3 cDNA is represented in the genomic sequence AE003536 and in the EST clone AT29009. The NXF3 clone used in Figure 2B corresponds to nt 218264–219265 of the genomic sequence AE003536. An *nxf4* gene prediction can be found in the Flybase (gene CG14604) and partially overlaps with the EST (AT07692). Sequencing the entire insert present in this EST clone, however, showed that it corresponds to nt 261141 to 262142 of the genomic sequence AE003672.2 and that the 5′ end of the predicted *nxf4* gene needs to be redefined. In our studies, the insert present in the EST clone (AT07692) was used directly for further studies.

Plasmids, recombinant protein expression, and in vitro binding assays

Plasmids allowing the expression of HA-tagged NXF1, NXF1 fragment 137–672, NXF2, or p15 in SL2 cells, were generated by inserting the corresponding cDNAs into a pBS-based vector containing the *Drosophila* actin promoter and the BgH1 terminator (pBSact). Plasmids allowing the expression of glutathione S-transferase (GST) fusions of NXF1, NXF2, or p15 in *Escherichia coli* were generated by inserting the corresponding cDNAs between the *EcoR*I and *Not*I sites of pGEX5X-3 (NXF1137–672), the *Nco*I and the *Eco*RI sites of pGEXCS (NXF2), or the *Nco*I and *Bam*HI sites present in pGEXCS (p15). A plasmid encoding a GST fusion of NXF2 amino acids 1–326 was made by digesting plasmid pGEXCS-NXF2 with *Sph*I and *EcoR*I followed by recircularization. Plasmids encoding Hs p15 or TAP and its derivatives have been described previously (Braun et al., 2001; Bachi et al., 2000). Recombinant proteins were expressed in *E. coli* BL21 (DE3) LysS and purified as previously described (Grüter et al., 1998). For the generation of [^{35}S]labeled proteins, the combined in vitro transcription-translation (TnT) kit from Promega was used. GST pull-down experiments were performed as described (Bachi et al., 2000).

RNA isolation, RT-PCR, and northern blots

To determine the expression pattern of human NXFs, a multiple tissue northern blot (Origene) was consecutively hybridized using probes comprising the first 0.3 kb of the corresponding coding regions. Slot blot analysis confirmed that these probes do not cross-hybridize.

Total RNA was isolated from cultured cells or Dm embryos using TRIzol Reagent (Life Technologies). Reverse transcription was performed with AMV reverse transcriptase (Promega) on 2 μg of total RNA and was primed with oligo(dT)$_{15}$. One-tenth of these reactions served as template in the subsequent PCR reactions performed using specific primers.

For northern blotting, total RNA was separated in denaturing formaldehyde agarose gels and blotted onto a positively charged nylon membrane (GeneScreen Plus, NEN Life Science). [^{32}P]labeled probes were generated by random priming using standard methods or by linear PCR using the Strip-EZ PCR kit (Ambion). Hybridizations were carried out in ULTRAhyb solution (Ambion). Slot blot assays confirmed that the probes used do not cross-hybridize and that all probes exhibit a detection limit of less than 2 pg.

A plasmid containing the complete coding region of rp49 in pOT2 was provided by Heinrich Jasper (EMBL, Germany). Plasmids comprising the first 1,200 bp of HSP70 and the last 1,300 bp of HSP83 cDNAs were kindly provided by Carl Wu (Bethesda, USA).

Cell culture and RNA interference

SL2 cells were propagated at 25 °C in Schneider's *Drosophila* medium supplemented with 10% foetal bovine serum, 100 U/mL penicillin and 100 μg/mL streptomycin. dsRNAi was performed essentially as described by Clemens et al. (2000). NXF1 and NXF3 dsRNAs correspond to a fragment comprising amino acids 137–354 and 166–382, respectively. NXF2, eIF4G, and GFP (enhanced GFP from vector pEGFP-C1) dsRNA correspond each to the first 650 bp of the coding regions. p15 dsRNA corresponds to the first 350 nt of p15 coding region. Fifteen micrograms of dsRNA were used per 6-well dish containing ~10^6 cells. NXF4 dsRNA correspond to nt 261148–261798 of the genomic sequence AE003672.2.

Preparation of total cell extracts and western blotting

Total-cell extracts were prepared by washing the cells with PBS and resuspending them directly in SDS-sample buffer at a concentration of ~30,000 cells/μL. Extracts were sonicated to shear genomic DNA. Typically 5–15 μL of this extract was used for western blot analysis. Rabbit polyclonal antibodies raised to recombinant GST-NXF1 (fragment 137–672) and GST-NXF2 (residues 1–326) were diluted 1:500. A rat polyclonal antibody was raised to Dm p15 expressed in *E. coli* as a hexa-histidine fusion protein. This antiserum was diluted 1:750. Anti-eIF4G antibodies were diluted 1:5,000. Bound primary antibody was detected with alkaline-phosphatase coupled anti-rabbit or anti-rat antibodies (Western-Star kit from Tropix).

In vivo protein labeling

SL2 cells transfected with dsRNA (~2×10^6) were transferred to 15-mL Falcon tubes, washed once with serum-free M3 *Drosophila* medium lacking methionine (Sigma), and incubated in 200 μL of this medium for 20 min at 25 °C. After this preincubation period, 200 μL of methionine-free medium supplemented with 125 μCi/mL of [^{35}S]methionine (Pro-mix in vitro cell labeling mix; Amersham) were added. Cells were either kept at 25 °C or immediately shifted to 37 °C by immersing the tubes in a water bath. After 1 h, cells were washed twice with ice-cold PBS and directly resuspended in 100 μL SDS sample buffer. Aliquots of 25 μL were analyzed by SDS-PAGE and fluorography.

Fluorescence in situ hybridization (FISH) and immunofluorescence

SL2 cells were allowed to adhere to poly-D-Lysine-coated coverslips for 2 min, washed once in PBS, and fixed with 3.7% paraformaldehyde in PBS for 10 min. After fixation, cells were washed in PBS, permeabilized for 10 min with PBS containing 0.5% Triton X-100 and washed again with PBS.

To detect poly(A)$^+$ RNA, cells were incubated for 15 min at 37 °C in prehybridization buffer (2× SSC, 20% formamide, 0.2% BSA, 1 mg/mL of total yeast tRNA). For hybridization, the coverslips were transferred to a humidified chamber and covered with 20 μL of hybridization buffer (prehybridization buffer plus 10% dextran sulfate) supplemented with 0.1 pmol/μL oligo(dT)$_{50}$ fluorescently end labeled with Cy3 molecules. The cells were hybridized for 2–3 h at 37 °C and washed successively two times for 5 min with 2× SSC/20% formamide (at 42 °C), 2× SSC (at 42 °C), 1× SSC, and PBS. Subsequent indirect immunofluorescence with mAb414 (BaBco) antibodies diluted 1:1,000 was performed as described (Almeida et al., 1998). Alexa488-coupled goat secondary antibody (Molecular probes) was used in a dilution of 1:750. Alternatively, nuclear envelopes were stained with Alexa Fluor488-WGA conjugates (dilution 1:1,500). DNA was stained with Hoechst 33342 (Molecular probes). Cells were mounted using Fluoromount-G (Southern Biotechnology Associates, Inc.).

For FISH analysis of *hsp70*, *hsp83*, and *rp49* mRNA digoxigenin-labeled antisense RNA probes were synthesized using the DIG RNA labeling mix and T3/T7/SP6 RNA polymerases (Roche). Probes were diluted 1:100 from stocks at 0.05–0.1 μg/μL. Hybridizations were performed as described above with the following modifications. After permeabilization, cells were washed for 5 min with 2× SSC/50% formamide and then incubated for 15 min in prehybridization buffer (2× SSC, 50% formamide, 50 mM sodium phosphate, pH 7.3, 300 μg/mL sonicated single-stranded DNA) at 58 °C. Hybridization was done overnight at 58 °C with 25 μL hybridization buffer per coverslip (prehybridization buffer plus 10% dextrane sulphate and 10 mM ribonucleoside vanadyl complex) containing the digoxigenin-labeled RNA probe. Cells were washed three times for 10 min with 2× SSC/50% formamide, twice for 15 min with 2× SSC, and twice for 10 min with 1× SSC at 58 °C. To detect the digoxigenin-labeled probes, cells were washed with PBS and incubated with a polyclonal sheep anti-digoxigenin antibody (1:100 in PBT; Roche). After several washes with PBT, cells were incubated with a Cy3-conjugated rabbit anti-sheep antibody (1:250 in PBT; Jackson ImmunoResearch), washed with PBS, and fixed and mounted as above. Images were taken with a confocal laser scanning microscope (LSM 510 from Carl Zeiss).

To investigate the subcellular localization of NXF1, NXF2, and p15, SL2 cells (~2×10^6) were transfected using the calcium-phosphate method with 2 μg of plasmid DNA encoding HA-tagged versions of the proteins. Sixty hours after transfection, indirect immunofluorescence was performed as for the FISH experiments. Cells were double labeled with an anti-HA antibody (bAbco) and an affinity purified polyclonal antibody (KJ58; Rodrigues et al., 2001) that detects Dm REF1.

ACKNOWLEDGMENTS

We are grateful to Ilan Davis, Christopher A. Korey, David Van Vactor, and Gavin Wilkie for communicating results prior to publication. The technical assistance of Michaela Rode is gratefully acknowledged. We thank José Manuel Sierra for the kind gift of anti-eIF4G antibodies, Rolando Rivera-Pomar for a plasmid encoding eIF4G, Carl Wu for providing various heat-shock cDNA clones, Stephen Cohen for Clone 8 cells, Harald Saumweber for Kc cells, and Mikita Suyama for gene prediction and sequence analysis. This study was supported by the European Molecular Biology Organization (EMBO).

Received August 17, 2001; returned for revision September 17, 2001; revised manuscript received September 27, 2001

REFERENCES

Almeida F, Saffrich R, Ansorge W, Carmo-Fonseca M. 1998. Microinjection of anti-coilin antibodies affects the structure of coiled bodies. *J Cell Biol 142*:899–912.

Bachi A, Braun IC, Rodrigues JP, Pante N, Ribbeck K, von Kobbe C, Kutay U, Wilm M, Görlich D, Carmo-Fonseca M, Izaurralde E. 2000. The C-terminal domain of TAP interacts with the nuclear pore complex and promotes export of specific CTE-bearing RNA substrates. *RNA 6*:136–158.

Bear J, Tan W, Zolotukhin AS, Tabernero C, Hudson EA, Felber BK. 1999. Identification of novel import and export signals of human TAP, the protein that binds to the CTE element of the type D retrovirus mRNAs. *Mol Cell Biol 19*:6306–6317.

Black BE, Holaska JM, Lévesque L, Ossareh-Nazari B, Gwizdek C, Dargemont C, Paschal BM. 2001. NXT1 is necessary for the terminal step of Crm1-mediated nuclear export. *J Cell Biol 152*: 141–156.

Black BE, Levesque L, Holaska JM, Wood TC, Paschal BM. 1999. Identification of an NTF2-related factor that binds Ran-GTP and regulates nuclear protein export. *Mol Cell Biol 19*:8616–8624.

Braun IC, Herold A, Rode M, Conti E, Izaurralde E. 2001. Overexpression of TAP/p15 heterodimers bypasses nuclear retention and stimulates nuclear mRNA export. *J Biol Chem 276*:20536–20543.

Clemens JC, Worby CA, Simonson-Leff N, Muda M, Maehama T, Hemmings BA, Dixon JE. 2000. Use of double-stranded RNA interference in *Drosophila* cell lines to dissect signal transduction pathways. *Proc Natl Acad Sci USA 97*:6499–6503.

Conti E, Izaurralde E. 2001. Nucleocytoplasmic transport enters the atomic age. *Curr Opin Cell Biol 3*:310–319.

Echalier G. 1997. *Drosophila cells in culture*. San Diego, California: Academic Press.

Fribourg S, Braun IC, Izaurralde E, Conti E. 2001. Structural basis for the recognition of a nucleoporin FG repeat by the NTF2-like domain of the TAP/p15 mRNA nuclear export factor. *Mol Cell 8*: 645–656.

Grüter P, Tabernero C, von Kobbe C, Schmitt C, Saavedra C, Bachi A, Wilm M, Felber BK, Izaurralde E. 1998. TAP, the human homolog of Mex67p, mediates CTE-dependent RNA export from the nucleus. *Mol Cell 1*:649–659.

Guzik BW, Levesque L, Prasad S, Bor YC, Black BE, Paschal BM, Rekosh D, Hammarskjold ML. 2001. NXT1 (p15) is a crucial cellular cofactor in TAP-dependent export of intron-containing RNA in mammalian cells. *Mol Cell Biol 7*:2545–2554.

Herold A, Suyama M, Rodrigues JP, Braun IC, Kutay U, Carmo-Fonseca M, Bork P, Izaurralde E. 2000. TAP/NXF1 belongs to a multigene family of putative RNA export factors with a conserved modular architecture. *Mol Cell Biol 20*:8996–9008.

Hilleren P, Parker R. 2001. Defects in the mRNA export factors Rat7p, Gle1p, Mex67p, and Rat8p cause hyperadenylation during 3′-end formation of nascent transcripts. *RNA 7*:753–764.

Hurt E, Strässer K, Segref A, Bailer S, Schlaich N, Presutti C, Tollervey D, Jansen R. 2000. Mex67p mediates nuclear export of a variety of RNA polymerase II transcripts. *J Biol Chem 275*:8361–8365.

Jensen TH, Patricio K, McCarthy T, Rosbash M. 2001. A block to mRNA nuclear export in *S. cerevisiae* leads to hyperadenylation of transcripts that accumulate at the site of transcription. *Mol Cell 7*:887–898.

Jun L, Frints S, Duhamel H, Herold A, Abad-Rodrigues J, Dotti C, Izaurralde E, Marynen P, Froyen G. 2001. NXF5, a novel member of the nuclear RNA export factor family, is lost in a male patient with a syndromic form of mental retardation. *Curr Biol 11*:1381–1391.

Kadowaki T, Hitomi M, Chen S, Tartakoff AM. 1994. Nuclear mRNA accumulation causes nucleolar fragmentation in yeast mtr2 mutant. *Mol Biol Cell 11*:1253–1263.

Kang Y, Bogerd HP, Cullen BR. 2000. Analysis of cellular factors that mediate nuclear export of RNAs bearing the Mason-Pfizer monkey virus constitutive transport element. *J Virol 13*:5863–5871.

Katahira J, Strässer K, Podtelejnikov A, Mann M, Jung JU, Hurt E. 1999. The Mex67p-mediated nuclear mRNA export pathway is conserved from yeast to human. *EMBO J 18*:2593–2609.

Korey CA, Wilkie G, Davis I, Van Vactor D. 2001. *small bristles*, DmNXF1, is required for the morphogenesis of multiple tissues during *Drosophila* development. *Genetics*. In press.

Liker E, Fernandez E, Izaurralde E, Conti E. 2000. The structure of the mRNA nuclear export factor TAP reveals a *cis* arrangement of a non-canonical RNP domain and a leucine-rich-repeat domain. *EMBO J 19*:5587–5598.

Mattaj IW, Englmeier L. 1998. Nucleocytoplasmic transport: The soluble phase. *Annu Rev Biochem 67*:265–306.

Nakielny S, Dreyfuss G. 1999. Transport of proteins and RNAs in and out of the nucleus. *Cell 99*:677–690.

Ossareh-Nazari B, Maison C, Black BE, Levesque L, Paschal BM, Dargemont C. 2001. RanGTP-Binding Protein NXT1 facilitates nuclear export of different classes of RNA in vitro. *Mol Cell Biol 20*:4562–4571.

Pasquinelli AE, Ernst RK, Lund E, Grimm C, Zapp ML, Rekosh D, Hammarskjold M-L, Dahlberg JE. 1997. The constitutive transport element (CTE) of Mason-Pfizer Monkey Virus (MPMV) accesses an RNA export pathway utilized by cellular messenger RNAs. *EMBO J 16*:7500–7510.

Rodrigues JP, Rode M, Gatfield D, Blencowe BJ, Carmo-Fonseca M, Izaurralde E. 2001. REF proteins mediate the export of spliced and unspliced mRNAs from the nucleus. *Proc Natl Acad Sci USA 98*:1030–1035.

Saavedra CA, Felber BK, Izaurralde E. 1997. The simian retrovirus-1 constitutive transport element CTE, unlike HIV-1 RRE, utilizes factors required for cellular RNA export. *Curr Biol 7*:619–628.

Santos-Rosa H, Moreno H, Simos G, Segref A, Fahrenkrog B, Panté N, Hurt E. 1998. Nuclear mRNA export requires complex formation between Mex67p and Mtr2p at the nuclear pores. *Mol Cell Biol 18*:6826–6838.

Segref A, Sharma K, Doye V, Hellwig A, Huber J, Lührmann R, Hurt E. 1997. Mex67p, a novel factor for nuclear mRNA export binds to both poly(A)+ RNA and nuclear pores. *EMBO J 16*:3256–3271.

Strässer K, Bassler J, Hurt E. 2000. Binding of the Mex67p/Mtr2p heterodimer to FXFG, GLFG, and FG repeat nucleoporins is essential for nuclear mRNA export. *J Cell Biol 150*:695–706.

Stutz F, Bachi A, Doerks T, Braun IC, Séraphin B, Wilm M, Bork P, Izaurralde E. 2000. REF, an evolutionary conserved family of hnRNP-like proteins, interacts with TAP/Mex67p and participates in mRNA nuclear export. *RNA 6*:638–650.

Suyama M, Doerks T, Braun IC, Sattler M, Izaurralde E, Bork P. 2000. Prediction of structural domains of TAP reveals details of its interaction with p15 and nucleoporins. *EMBO Rep 1*:53–58.

Tan W, Zolotukhin AS, Bear J, Patenaude DJ, Felber BK. 2000. The mRNA export in *C. elegans* is mediated by Ce NXF1, an orthologue of human TAP/NXF1 and *S. cerevisiae* Mex67p. *RNA 6*:1762–1772.

Vainberg IE, Dower K, Rosbash M. 2000. Nuclear export of heat shock and non-heat-shock mRNA occurs via similar pathways. *Mol Cell Biol 20*:3996–4005.

Wilkie GS, Zimyanin V, Kirby R, Korey CA, Francis-Lang H, Sullivan W, Van Vactor D, Davis I. 2001. *Small bristles*, the *Drosophila* ortholog of human TAP/NXF1 and yeast Mex67p, is essential for mRNA nuclear export in all tissues throughout development. *RNA 7*:1781–1792.

Yang J, Bogerd HP, Wang PJ, Page DC, Cullen BR. 2001. Two closely related human nuclear export factors utilize entirely distinct export pathways. *Mol Cell 8*:397–406.

Yoon DW, Lee H, Seol W, DeMaria M, Rosezweig M, Jung JU. 1997. Tap: A novel cellular protein that interacts with tip of herpes virus saimiri and induces lymphocyte aggregation. *Immunity 6*:571–582.

Yost HJ, Lindquist S. 1986. RNA splicing is interrupted by heat shock and is rescued by heat shock protein synthesis. *Cell 45*:185–193.